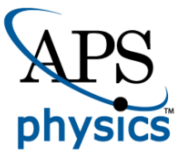

Nonhelical Inverse Transfer of a Decaying Turbulent Magnetic Field

Axel Brandenburg, Tina Kahniashvili, and Alexander G. Tevzadze

Phys. Rev. Lett. **114**, 075001 — Published 19 February 2015

DOI: 10.1103/PhysRevLett.114.075001

Nonhelical inverse transfer of a decaying turbulent magnetic field

Axel Brandenburg,[1,2,*] Tina Kahniashvili,[3,4,5,†] and Alexander G. Tevzadze[6,‡]

[1] *Nordita, KTH Royal Institute of Technology and Stockholm University, Roslagstullsbacken 23, 10691 Stockholm, Sweden*
[2] *Department of Astronomy, AlbaNova University Center, Stockholm University, 10691 Stockholm, Sweden*
[3] *The McWilliams Center for Cosmology and Department of Physics, Carnegie Mellon University, 5000 Forbes Ave, Pittsburgh, PA 15213, USA*
[4] *Department of Physics, Laurentian University, Ramsey Lake Road, Sudbury, ON P3E 2C, Canada*
[5] *Abastumani Astrophysical Observatory, Ilia State University, 3-5 Cholokashvili Ave, Tbilisi, GE-0194, Georgia*
[6] *Faculty of Exact and Natural Sciences, Tbilisi State University, 1 Chavchavadze Ave., Tbilisi, 0128, Georgia*

(Dated: Received 8 April 2014; January 20, 2015; Revision: 1.66)

In the presence of magnetic helicity, inverse transfer from small to large scales is well known in magnetohydrodynamic (MHD) turbulence and has applications in astrophysics, cosmology, and fusion plasmas. Using high resolution direct numerical simulations of magnetically dominated self-similarly decaying MHD turbulence, we report a similar inverse transfer even in the absence of magnetic helicity. We compute for the first time spectral energy transfer rates to show that this inverse transfer is about half as strong as with helicity, but in both cases the magnetic gain at large scales results from velocity at similar scales interacting with smaller-scale magnetic fields. This suggests that both inverse transfers are a consequence of a universal mechanisms for magnetically dominated turbulence. Possible explanations include inverse cascading of the mean squared vector potential associated with local near two-dimensionality and the shallower k^2 subinertial range spectrum of kinetic energy forcing the magnetic field with a k^4 subinertial range to attain larger-scale coherence. The inertial range shows a clear k^{-2} spectrum and is the first example of fully isotropic magnetically dominated MHD turbulence exhibiting weak turbulence scaling.

PACS numbers: 98.70.Vc, 98.80.-k

The nature of magnetohydrodynamic (MHD) turbulence has received significant attention in recent years [1]. Whenever plasma is ionized, it is electrically conducting and Kolmogorov's turbulence theory [2] has to be replaced by an appropriate theory for MHD turbulence [3]. This becomes relevant under virtually all astrophysical circumstances. However, the universal character of MHD turbulence is debated and several fundamental questions remain unanswered: how do kinetic and magnetic energy spectra look like and are they similar? How does this depend on the magnetic Prandtl number, $\mathrm{Pr_M}=\nu/\eta$, i.e., the ratio of kinematic viscosity and magnetic diffusivity? What is the role of the Alfvén effect, i.e., how does the presence of a finite Alfvén speed v_A enter the expression for the turbulent energy spectrum?

If the spectral properties of MHD turbulence are governed solely by the rate of energy transfer ϵ, we know from dimensional arguments that the spectrum must scale as $E(k)\sim\epsilon^{2/3}k^{-5/3}$ with wavenumber k. However, MHD turbulence becomes increasingly anisotropic toward small scales [4], so the spectrum $E(k_\perp,k_\parallel)$ depends on the wavenumbers perpendicular and parallel to the magnetic field $\boldsymbol{B}$, and is essentially given by $\epsilon^{2/3}k_\perp^{-5/3}$, so most of the energy cascades perpendicular to $\boldsymbol{B}$.

In the case of forced turbulence, direct numerical simulations (DNS) show similar spectra both with imposed [1] and dynamo-generated [5] fields. However, when $\boldsymbol{B}$ is decaying, the result depends on the value of the initial ratio $v_\mathrm{A}/u_\mathrm{rms}$ of root mean square (rms) Alfvén speed to rms turbulent velocity. Recent DNS [6] found numerical evidence for three different scalings: Iroshnikov–Kraichnan scaling [7] proportional to $(\epsilon v_\mathrm{A})^{1/2}k^{-3/2}$ for $v_\mathrm{A}/u_\mathrm{rms}=0.9$, Goldreich–Sridhar scaling [4] proportional to $\epsilon^{2/3}k_\perp^{-5/3}$ for $v_\mathrm{A}/u_\mathrm{rms}=1.3$, and weak turbulence scaling [8] proportional to $(\epsilon v_\mathrm{A}k_\parallel)^{1/2}k_\perp^{-2}$ for $v_\mathrm{A}/u_\mathrm{rms}=2.0$; see Ref. [9] for a comparison of these three scalings. However, their physical interpretation is subject to criticism in that dynamic alignment between $\boldsymbol{u}$ and $\boldsymbol{B}$ can be responsible for the shallower $k^{-3/2}$ scaling [10] and the k^{-2} scaling could also be caused by a dominance of discontinuities [11].

It is usually taken for granted that for non-helical turbulence, energy is cascading toward small scales. An inverse cascade has so far only been found for helical turbulence [3, 12] and was confirmed in DNS [13–15]. It is evident that this requires significant scale separation, $k_0/k_1\gg1$, where k_0 is the wavenumber of the peak of the spectrum and $k_1=2\pi/L$ is the minimal wavenumber of the domain of size L. Since an inverse transfer was not expected to occur in the absence of helicity, most previous work did not allow for $k_0/k_1\gg1$. However, when k_0/k_1 is moderate, some inverse cascading was found [14]. The present work shows that this behavior is genuine and

*Electronic address: brandenb@nordita.org
†Electronic address: tinatin@phys.ksu.edu
‡Electronic address: aleko@tevza.org

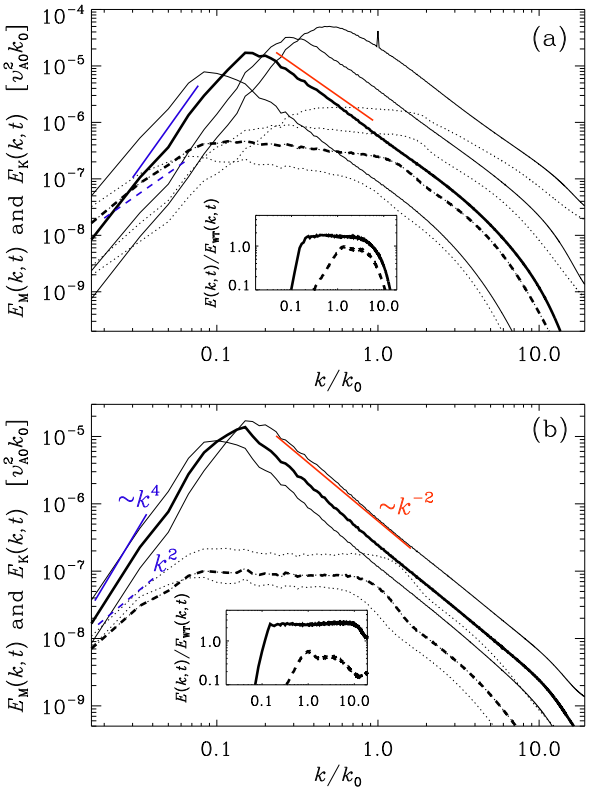

FIG. 1: (Color online) (a) Magnetic (solid lines) and kinetic (dashed lines) energy spectra for Run A at times $t/\tau_A = 18$, 130, 450, and 1800; the time $t/\tau_A = 450$ is shown as bold lines. The straight lines indicate the slopes k^4 (solid, blue), k^2 (dashed, blue), and k^{-2} (red, solid). (b) Same for Run B, at $t/\tau_A = 540$, 1300, and 1800, with $t/\tau_A = 1300$ shown as bold lines. The insets show E_M and E_K compensated by E_{WT}.

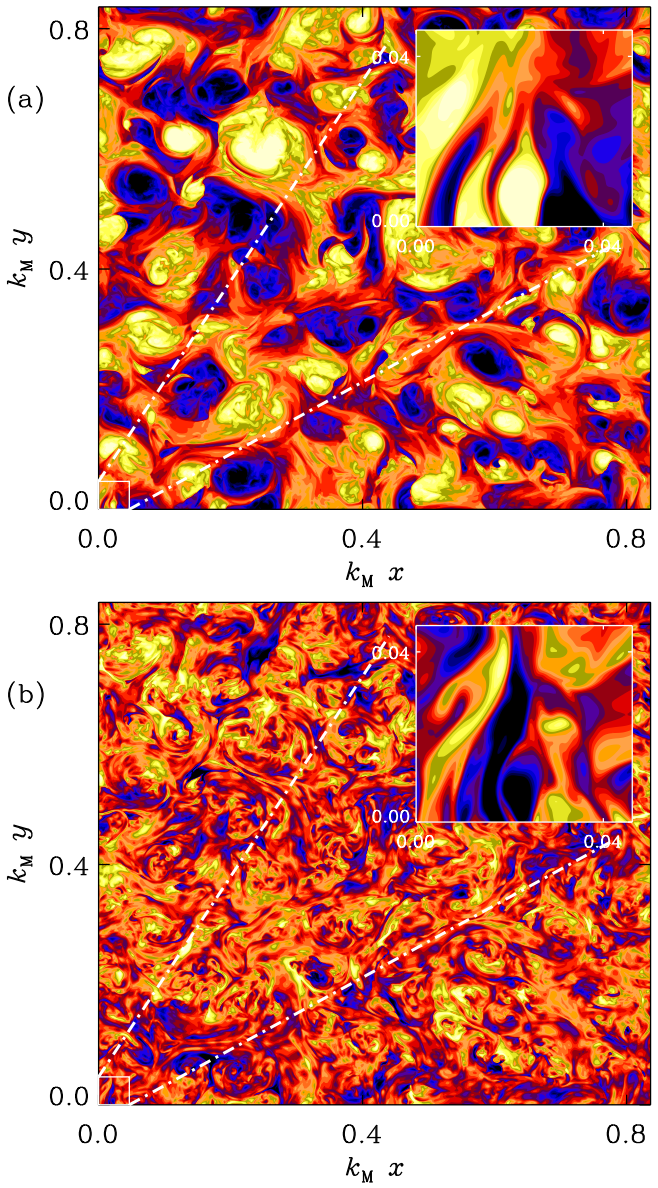

FIG. 2: (Color online) Contours of (a) $B_z(x,y)$ and (b) $u_z(x,y)$ for Run A. The insets show a zoom into the small square in the lower left corner.

more pronounced at higher resolution, larger Reynolds numbers and larger k_0/k_1.

We solve the compressible MHD equations for $\boldsymbol{u}$, the gas density ρ at constant sound speed c_s, and the magnetic vector potential $\boldsymbol{A}$, so $\boldsymbol{B} = \boldsymbol{\nabla} \times \boldsymbol{A}$. Following our earlier work [16–18], we initialize our decaying DNS by restarting them from a snapshot of a driven DNS, where a random forcing was applied in the evolution equation for $\boldsymbol{A}$ rather than $\boldsymbol{u}$ [19]. To allow for sufficient scale separation, we take $k_0/k_1 = 60$. We use the Pencil Code [29] at a resolution of 2304^3 meshpoints on 9216 processors. The code uses sixth order finite differences and a third order accurate time stepping scheme.

Our magnetic and kinetic energy spectra are normalized such that $\int E_M(k,t)\,dk = \mathcal{E}_M(t) = v_A^2/2$ and $\int E_K(k,t)\,dk = \mathcal{E}_K(t) = u_{rms}^2/2$ are magnetic and kinetic energies per unit mass. The magnetic integral scale is defined as $\xi_M = k_M^{-1}(t) = \int k^{-1} E_M(k,t)\,dk/\mathcal{E}_M(t)$. Time is given in initial Alfvén times $\tau_A = (v_{A0}k_0)^{-1}$, where $v_{A0} = v_A(0)$. In Fig. 1 we show $E_M(k,t)$ and $E_K(k,t)$ for Runs A and B (restarted from A at $t/\tau_A = 450$) with $\mathrm{Pr_M} = 1$ and 10, respectively, and in Fig. 2 slices $B_z(x,y)$ and $u_z(x,y)$ at $z = 0$ at the last time Run A. We find an inertial range with weak turbulence scaling,

$$E_{WT}(k,t) = C_{WT}(\epsilon v_A k_M)^{1/2} k^{-2}, \qquad (1)$$

where $k_M^{-1}(t) = \int k^{-1} E_M(k,t)\,dk/\mathcal{E}_M(t)$ is the integral scale and k_M has been used in place of $k_\parallel$. The prefactor is $C_{WT} \approx 1.9$ for $\mathrm{Pr_M} = 1$ and ≈ 2.4 for $\mathrm{Pr_M} = 10$; see the insets. In agreement with earlier work [3, 17], $\mathcal{E}_M$ decays like t^{-1}.

At small wavenumbers the k^4 and k^2 subinertial ranges respectively for $E_M(k,t)$ and $E_K(k,t)$ are carried over from the initial conditions. The k^4 Batchelor spectrum is in agreement with the causality requirement [30, 31] for

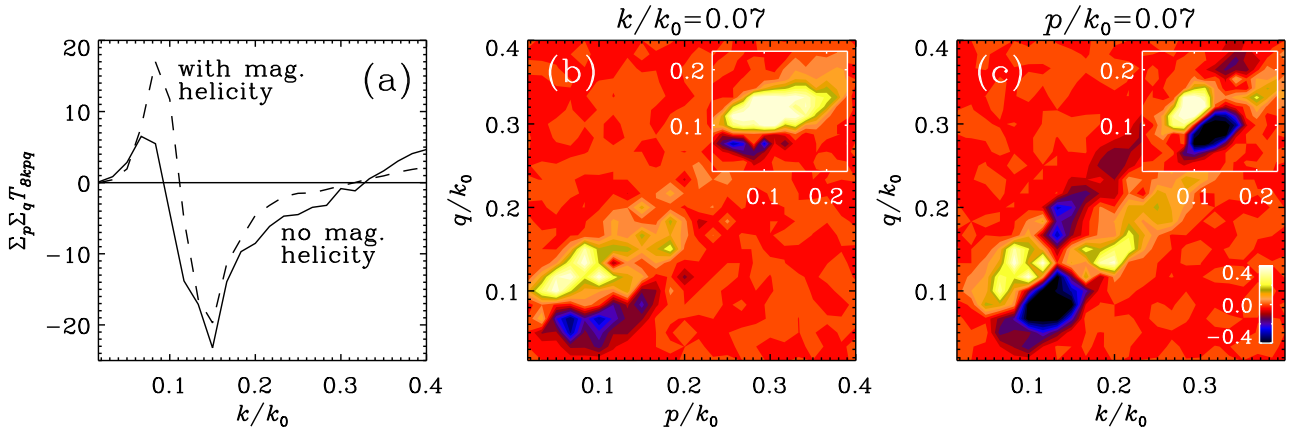

FIG. 3: (Color online) Spectral transfer function T_{kpq}, (a) as a function of k and summed over all p and q, (b) as a function of p and q for $k/k_1 = 4$, and (c) as a function of k and q for $p/k_1 = 4$. The dashed line in (a) and the insets in (b) and (c) show the corresponding case for a DNS with helicity; both for $\mathrm{Pr_M} = 1$.

the divergence-free vector field $\boldsymbol{B}$. The velocity is driven entirely by the magnetic field (no kinetic forcing) and follows a white noise spectrum, $E_\mathrm{K}(k) \propto k^2$ [31]. The resulting difference in the scaling implies that, although magnetic energy dominates over kinetic, the two spectra must cross at sufficiently small wavenumbers. This idea may also apply to incompressible [32] and relativistic [33] simulations, where inverse nonhelical transfer has recently been confirmed.

To quantify the nature of inverse transfer we show in Fig. 3 representations of the spectral transfer function $T_{kpq} = \langle \boldsymbol{J}^k \cdot (\boldsymbol{u}^p \times \boldsymbol{B}^q) \rangle$ and compare with the corresponding helical case of Ref. [18], but with 1024^3 mesh points and at a comparable time. Here, the superscripts indicate the radius of a shell in wavenumber space of Fourier filtered vector fields; see Ref. [15] for such an analysis in driven helical turbulence. The transfer function T_{kpq} quantifies the gain of magnetic energy at wavenumber k from interactions of velocities at wavenumber p and magnetic fields at wavenumber q. Fig. 3(a) shows a gain for $k/k_0 < 0.1$, which is about half of that for the helical case. The corresponding losses for $k/k_0 > 0.1$ are about equal in the two cases. In both cases, the magnetic gain at $k/k_0 = 0.07 = 4/60$ results from $\boldsymbol{u}^p$ with $0 < p/k_0 < 0.2$ interacting with $\boldsymbol{B}^q$ at $q/k_0 > 0.1$; see the light yellow shades in Fig. 3(b). Note that work done by the Lorentz force is $\langle \boldsymbol{u}^p \cdot (\boldsymbol{J}^k \times \boldsymbol{B}^q) \rangle = -T_{kpq}$. Thus, negative values of T_{kpq} quantify the gain of *kinetic* energy at wavenumber p from interactions of magnetic fields at wavenumbers k and q. Blue dark shades in Fig. 3(c) indicate therefore that the gain of kinetic energy at $p/k_0 = 0.07$ results from magnetic interactions at wavenumbers k and q of around $0.1\,k_0$. These results support the interpretation that the increase of spectral power at large scales is similar to the inverse transfer in the helical case; see [19] for information concerning the *total* energy transfer.

To exclude that the inverse energy transfer is a consequence of the invariance of magnetic helicity, $\mathcal{H}_\mathrm{M}(t) = \langle \boldsymbol{A} \cdot \boldsymbol{B} \rangle$, we compare ξ_M with its lower bound $\xi_\mathrm{M}^\mathrm{min} = |\mathcal{H}_\mathrm{M}|/2\mathcal{E}_\mathrm{M}$ [17]; see Fig. 4. In nonhelical MHD turbulence, ξ_M is known to grow like $t^{1/2}$ [3, 17]. Even though the initial condition was produced with nonhelical plane wave forcing, we find $\mathcal{H}_\mathrm{M} \neq 0$ due to fluctuations. Since $\mathcal{H}_\mathrm{M}$ is conserved and $\mathcal{E}_\mathrm{M}$ decays like t^{-1} [3, 17], $\xi_\mathrm{M}^\mathrm{min}$ grows linearly and faster than $\xi_\mathrm{M} \sim t^{1/2}$, so they will meet at $t/\tau_\mathrm{A} = 10^5$ and then continue to grow as $t^{-2/3}$ [3, 17], but at $t/\tau_\mathrm{A} = 10^3$ this cannot explain the inverse transfer. By contrast, we cannot exclude the possibility of the quasi two-dimensional mean squared vector potential, $\langle \boldsymbol{A}_\mathrm{2D}^2 \rangle$, being approximately conserved [19]. This could explain the $\xi_\mathrm{M} \sim t^{1/2}$ scaling and the inverse transfer if the flow was locally two-dimensional [34].

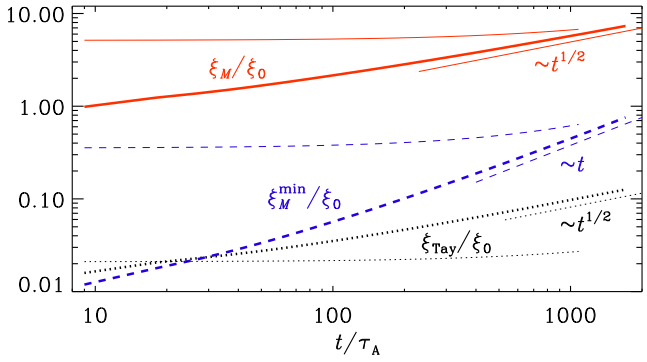

FIG. 4: Time evolution of $\xi_\mathrm{M} = k_\mathrm{M}^{-1}$ and $\xi_\mathrm{M}^\mathrm{min}$, as well as the Taylor microscale ξ_Tay. Fat (thin) lines are for Run A (B).

Since u_rms, v_A, and k_M are all proportional to $t^{-1/2}$, the decay is self-similar in such a way that the Reynolds and Lundquist numbers, $\mathrm{Re} = u_\mathrm{rms}/\nu k_\mathrm{M}$ and $\mathrm{Lu} = v_\mathrm{A}/\eta k_\mathrm{M}$, remain constant. Since $\mathcal{E}_\mathrm{K} \ll \mathcal{E}_\mathrm{M}$, the dissipated energy comes predominantly from $-d\mathcal{E}_\mathrm{M}/dt$, and yet a substantial fraction of it is used to drive kinetic

TABLE I: Comparison of relative dissipation rates, energies and other parameters for the two simulations discussed.

Run	$\mathrm{Pr_M}$	$v_{\rm A0}/c_{\rm s}$	$u_{\rm rms}/v_{\rm A}$	Lu	Re	$\epsilon_{\rm K}/\epsilon_{\rm M}$	$\epsilon_{\rm M}/\epsilon$	$\epsilon_{\rm K}/\epsilon$
A	1	0.15	0.36	700	230	0.52	0.66	0.34
B	10	0.03	0.21	6300	130	0.93	0.52	0.48

energy by performing work on the Lorentz force. Nevertheless, the viscous to magnetic dissipation ratio $\epsilon_{\rm K}/\epsilon_{\rm M}$ increases only by a factor of 1.8 as $\mathrm{Pr_M}$ increases from 1 to 10; see Table I. This is less than for kinetically driven MHD turbulence, where $\epsilon_{\rm K}/\epsilon_{\rm M} \propto \mathrm{Pr_M^{\it n}}$ with $n = 0.3$–0.7 [35]. Therefore, $\epsilon_{\rm M}$ is here larger than in driven MHD turbulence, where large Lu can still be tolerated. This suggests that Run B may be under-resolved, which might also explain why it did not reach asymptotic scaling in Fig. 4.

In summary, we have shown that inverse transfer is a ubiquitous phenomenon of both helical and non-helical MHD. For helical MHD, this has been well known for nearly four decades [12], but for nonhelical MHD there have only been some low resolution DNS [14, 18]. Our DNS confirm an early finding by Olesen [36] that this inverse transfer occurs for all initial spectra that are sufficiently steep. His argument applies to hydrodynamic and MHD turbulence if the two spectra are parallel to each other. In our case, however, owing to the shallower k^2 spectrum of kinetic energy, kinetic energy always dominates over magnetic at large enough length scales. Either this or the near-conservation of $\langle \boldsymbol{A}_{\rm 2D}^2 \rangle$ could be responsible for inverse transfer in magnetically dominated turbulence. This process is significant for cosmology and astrophysics [33], with applications not only to primordial magnetic fields, but also to ejecta from young stars, supernovae, and active galactic nuclei [37].

Our results support the idea of the weak turbulence k^{-2} scaling for strong magnetic field that is here for the first time globally isotropic and not an imposed one [38]. At small scales, however, approximate equipartition is still possible. The decay is slower than for usual MHD turbulence which is arguably governed by the Loitsyansky invariant [39]. Future investigations of the differences between these types of turbulence are warranted [19]. Interestingly, the extended plateau in the velocity spectrum around the position of the magnetic peak may be important for producing observationally detectable broad gravitational wave spectra [40].

We appreciate useful discussions with A. Neronov. Computing resources have been provided by the Swedish National Allocations Committee at the Center for Parallel Computers at the Royal Institute of Technology and by the Carnegie Mellon University Supercomputer Center. We acknowledge support from the Swedish Research Council grants 621-2011-5076 and 2012-5797, the European Research Council AstroDyn Project 227952, the Research Council of Norway FRINATEK grant 231444, the Swiss NSF grant SCOPES IZ7370-152581, the NSF grant AST-1109180, and the NASA Astrophysics Theory Program grant NNXlOAC85G. A.B. and A.T. acknowledge the hospitality of the McWilliams Center for Cosmology.

[1] W. H. Matthaeus, S. Ghosh, S. Oughton, and D. A. Roberts, J. Geophys. Res. **101**, 7619 (1996); J. Cho and E.T. Vishniac, Astrophys. J. **538**, 217 (2000); J. Maron and P. Goldreich, Astrophys. J. **554**, 1175 (2001).
[2] A. Kolmogorov, Dokl. Akad. Nauk SSSR, **30**, 301 (1941);
[3] D. Biskamp and W.-C. Müller, Phys. Rev. Lett. **83**, 2195 (1999).
[4] P. Goldreich and S. Sridhar, Astrophys. J. **438**, 763 (1995).
[5] N. E. L. Haugen, A. Brandenburg, and W. Dobler, Phys. Rev. E **70**, 016308 (2004).
[6] E. Lee, M. E. Brachet, A. Pouquet, P. D. Mininni, D. Rosenberg, Phys. Rev. E **81**, 016318 (2010).
[7] R. S. Iroshnikov, Sov. Astron. **7**, 566 (1963); R. H. Kraichnan, Phys. Fluids **8**, 1385 (1965).
[8] S. Galtier, S.V. Nazarenko, A.C. Newell, and A. Pouquet, J. Plasm. Phys. **63**, 447 (2000).
[9] A. Brandenburg and Å. Nordlund, Rep. Prog. Phys. **74**, 046901 (2011); W. H. Matthaeus, D. C. Montgomery, M. Wan, and S. Servidio, J. Turb. **13**, N37 (2012).
[10] J. Mason, F. Cattaneo, and S. Boldyrev, Phys. Rev. Lett. **97**, 255002 (2006).
[11] V. Dallas and A. Alexakis, Astrophys. J. **788**, L36 (2014).
[12] A. Pouquet, U. Frisch, and J. Léorat, J. Fluid Mech. **77**, 321 (1976).
[13] D. Balsara and A. Pouquet, Phys. Plasmas **6**, 89 (1999).
[14] M. Christensson, M. Hindmarsh, and A. Brandenburg, Phys. Rev. E **64**, 056405 (2001).
[15] A. Brandenburg, Astrophys. J. **550**, 824 (2001).
[16] T. Kahniashvili, A. Brandenburg, A. G. Tevzadze and B. Ratra, Phys. Rev. D **81**, 123002 (2010).
[17] A. G. Tevzadze, L. Kisslinger, A. Brandenburg and T. Kahniashvili, Astrophys. J. **759**, 54 (2012).
[18] T. Kahniashvili, A. G. Tevzadze, A. Brandenburg and A. Neronov, Phys. Rev. D **87**, 083007 (2013); note that in their Eq. (14), $\boldsymbol{v}/\eta$ should read $\partial \boldsymbol{v}/\partial\eta$.
[19] See Supplemental Material in arXiv:1404.2238, which includes Refs. [20–28].
[20] L. Campanelli, Eur. Phys. J. C **74**, 2690 (2014).
[21] C. Kalelkar and R. Pandit, Phys. Rev. E **69**, 046304 (2004).
[22] M. Christensson, M. Hindmarsh, and A. Brandenburg, Phys. Rev. E **64**, 056405 (2001).
[23] J. Baerenzung, H. Politano, Y. Ponty, and A. Pouquet, Phys. Rev. E **77**, 046303 (2008).
[24] A. Sen, P. D. Mininni, D. Rosenberg, and A. Pouquet, Phys. Rev. E **86**, 036319 (2012).
[25] A. Brandenburg, Å. Nordlund, R. F. Stein, and I. Torkelsson, Astrophys. J. **446**, 741 (1995).
[26] A. Brandenburg, Chaos, Solitons & Fractals **5**, 2025 (1995).
[27] A. Brandenburg, R. L. Jennings, Å. Nordlund, M. Rieutord, R. F. Stein, and I. Tuominen, J. Fluid Mech. **306**,

325 (1996).
[28] S. Sur, L. Pan, and E. Scannapieco, Astrophys. J. **790**, L9 (2014).
[29] http://pencil-code.googlecode.com/
[30] R. Durrer and C. Caprini, JCAP **0311**, 010 (2003).
[31] P. A. Davidson, *Turbulence* (Oxford Univ. Press, 2004).
[32] A. Berera and M. Linkmann, Phys. Rev. E **90**, 041003(R) (2014).
[33] J. Zrake, Astrophys. J. **794**, L26 (2014).
[34] A. Pouquet, J. Fluid Mech. **88**, 1 (1978).
[35] A. Brandenburg, Astrophys. J. **791**, 12 (2014).
[36] P. Olesen, Phys. Lett. B **398**, 321 (1997).
[37] A. M. Beck, K. Dolag, H. Lesch, and P. P. Kronberg, Mon. Not. R. Astron. Soc. **435**, 3575 (2013).
[38] J.C. Perez and S. Boldyrev, Astrophys. J. Lett. **672**, L61 (2008).
[39] P. A. Davidson, J. Turb. **1**, 006 (2000).
[40] T. Kahniashvili, L. Campanelli, G. Gogoberidze, Y. Maravin, and B. Ratra, Phys. Rev. D **78**, 123006 (2008).